

Hardware/Software Co-Exploration of Neural Architectures

Weiwen Jiang, *Student Member, IEEE*, Lei Yang, Edwin Sha, *Senior Member, IEEE*, Qingfeng Zhuge, Shouzhen Gu, Yiyu Shi, *Senior Member, IEEE*, and Jingtong Hu, *Member, IEEE*

Abstract—We propose a novel hardware and software co-exploration framework for efficient neural architecture search (NAS). Different from existing hardware-aware NAS which assumes a fixed hardware design and explores the *neural architecture search space* only, our framework simultaneously explores both the architecture search space and the *hardware design space* to identify the best neural architecture and hardware pairs that maximize both test accuracy and hardware efficiency. Such a practice greatly opens up the design freedom and pushes forward the Pareto frontier between hardware efficiency and test accuracy for better design tradeoffs. The framework iteratively performs a two-level (fast and slow) exploration. Without lengthy training, the fast exploration can effectively fine-tune hyperparameters and prune inferior architectures in terms of hardware specifications, which significantly accelerates the NAS process. Then, the slow exploration trains candidates on a validation set and updates a controller using the reinforcement learning to maximize the expected accuracy together with the hardware efficiency. Experiments on ImageNet show that our co-exploration NAS can find the neural architectures and associated hardware design with the same accuracy, 35.24% higher throughput, 54.05% higher energy efficiency and 136 \times reduced search time, compared with the state-of-the-art hardware-aware NAS.

Index Terms—Hardware-Software Co-Exploration, Neural Architecture Search, FPGA, Multi-Criteria Optimization

I. INTRODUCTION

The neural architecture search (NAS) has achieved great success to liberate human labor in the design of neural architectures for various tasks including image classification and language modeling [1]–[5]. Most recently, targeting a fixed hardware platform, the hardware-aware NAS [6]–[8] has been proposed to take into consideration the estimated timing performance (such as latency or throughput) in addition to accuracy (see Figure 1(a)).

All of the existing NAS frameworks explore the *architecture search space* only, without considering the hardware design freedom available in many cloud and edge computing applications. For instance, the cloud platforms (e.g. Amazon AWS [9] and Microsoft Azure [10]) employ Field Programmable Gate Array (FPGA) for neural network acceleration, while the edge computing platforms typically take the programmable FPGAs [11], [12] or Application-Specific Integrated Circuit (ASIC) [13], [14]. In addition to neural architecture design, those

W. Jiang and Y. Shi are with the Department of Computer Science and Engineering, University of Notre Dame, Notre Dame, IN 46556 (e-mail: wjiang2@nd.edu).

L. Yang and J. Hu are with the Department of Electrical and Computer Engineering, University of Pittsburgh, Pittsburgh, PA 15261.

E. H.-M. Sha, Q. Zhuge, and S. Gu are with the School of Computer Science and Software Engineering, East China Normal University, 200062 China

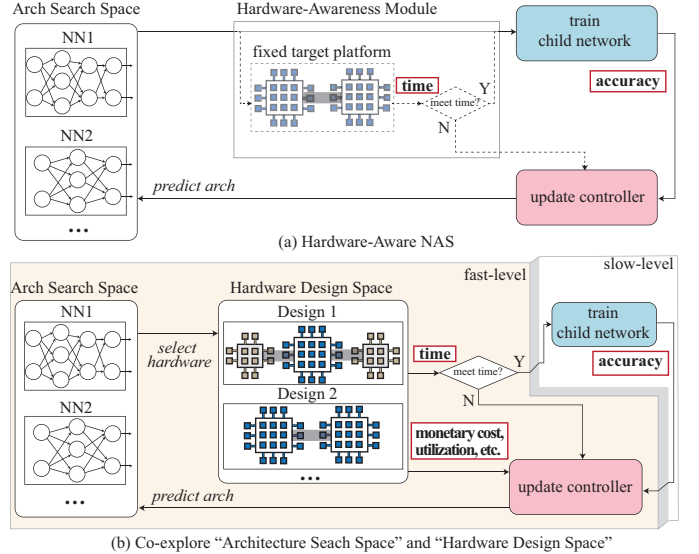


Figure 1. Comparison between (a) hardware-aware NAS; (b) the proposed hardware/software co-exploration NAS. The red rectangles convey the metrics that can be optimized in the exploration.

hardware platforms can also be programmed or even fully customized for the best performance, expanding a *hardware design space*.

Interestingly, the hardware design space is tightly coupled with the architecture search space, i.e., the best neural architecture depends on the hardware (hardware-aware NAS), and the best hardware depends on the neural architecture. It is therefore best to jointly explore both spaces to push forward the Pareto frontier between hardware efficiency and test accuracy for better design tradeoffs. This can be clearly seen from the example in Table I, where three designs on CIFAR-10 and Xilinx XC7Z015 FPGAs are presented: an optimized neural architecture for a fixed FPGA implementation through hardware-aware NAS (design A), the hardware of which is then further optimized through FPGA optimization (design B) [15], and a jointly optimized neural architecture and hardware through our co-exploration (design C). From the table, we can see that further optimizing the hardware for the architecture from hardware-aware NAS can lead to 45.45% higher throughput, 38.24% higher energy efficiency with the same accuracy. On the other hand, compared with such a sequential optimization strategy, our co-exploration approach can identify an architecture with higher accuracy and its tailor-made hardware with 16.33% and 28.80% improvements in

Table I

ON CIFAR-10 AND XILINX XC7Z015 FPGA: COMPARISONS OF THREE NEURAL ARCHITECTURE AND HARDWARE DESIGN PAIRS IN ACCURACY, THROUGHPUT, AND ENERGY EFFICIENCY (E.-E): A) OPTIMAL ARCHITECTURE ON A FIXED HARDWARE IMPLEMENTATION THROUGH HARDWARE-AWARE NAS; B) THE SAME ARCHITECTURE BUT WITH FURTHER FPGA OPTIMIZATION, AND C) A JOINTLY OPTIMIZED NEURAL ARCHITECTURE AND FPGA IMPLEMENTATION THROUGH OUR CO-EXPLORATION.

ID	Approach	Accuracy	Throughput (FPS)	E.-E (GOPS/W)
A	Hardware-Aware NAS	84.53%	16.2	0.84
B	Sequential Optimization	84.53%	29.7	1.36
C	Co-Exploration	85.19%	35.5	1.91

throughput and energy efficiency, respectively.

Specifically, our architecture search space and hardware design space co-exploration framework is shown in Figure 1(b). The proposed co-exploration can be built on any existing NAS framework [2], [8], [16], [17] by expanding it to delve into the hardware design space, where a two-level (fast and slow) exploration is iteratively conducted. In the fast exploration, the best hardware design is identified for the sampled neural architectures without lengthy training. The architectures with inferior hardware efficiency will be quickly pruned, which significantly accelerates the search process. Thereafter, the superior candidates are trained in the slow exploration for controller update using policy gradient reinforcement learning to explore the coupled architecture search space. The optimization objectives in the hardware design space can be varied according to the design specifications, such as area, monetary cost, energy efficiency, reliability, resource utilization, etc.

In order to illustrate our framework, we choose to use FPGA as a vehicle in this paper, as it has gradually become one of the most popular platforms to implement deep neural networks (DNNs) due to its programmability, high performance and energy efficiency, in particular for low-batch inferences [18], [19]. Our co-exploration concept and the general framework, however, can also be easily extended to other hardware platforms such as ASICs. Since timing performance on a single FPGA is limited by its restricted resource, it is prevalent to organize multiple FPGAs in a pipelined fashion [20]–[23] to provide high throughput (frame per second, FPS). In such a system, the pipeline efficiency is one of the most important metrics needing to be maximized, since it determines the hardware utilization as well as energy efficiency. As such, we use accuracy and pipeline efficiency to guide the exploration of the neural architecture space and hardware design space respectively, while satisfying a given throughput specifications (e.g., ≥ 30 FPS for the ordinary camera). Experimental results show that the co-exploration approach can significantly push forward the Pareto frontier. On ImageNet, the proposed co-exploration framework can identify architecture and hardware pairs to achieve the same accuracy, 35.42% higher throughput, 54.05% higher energy efficiency and 136 \times reduced search time, compared with the hardware-aware NAS.

II. BACKGROUND AND PROBLEM DEFINITION

A. Neural Architecture Search

Although the research on the automatic prediction of neural network architectures can trace back to the 1980s [24], after deep neural networks have achieved great success in AI domains, there have been growing interests in generating good neural architectures for the interested dataset recently. With the fact that the architectures are growing deeper, the search space expands exponentially, leading to more difficulties in exploring the search space. In existing work, there are two mainstreams of architecture search: (1) employing reinforcement learning [2], [3], [25], (2) applying evolutionary algorithms [4], [26], [27]. The basic idea is to iteratively update hyperparameters to generate better “child networks” in terms of accuracy.

Figure 1(a), without the hardware-aware module, illustrates a typically used reinforcement learning based neural architecture search (NAS) [2] framework. As shown in this figure, the RNN controller in NAS iteratively predicts child networks from architecture search space. These child networks will be trained on a held-out dataset to obtain its accuracy. Then, accuracy will be used to update the RNN controller.

Existing work has demonstrated that the automatically resulting architectures can achieve close or even higher accuracy to the best human-invented architectures [2], [3]. However, there are two important problems in searching architectures. First, the search process is inefficient. [2] reported that 20,000 networks were trained across 500 P100 GPUs over 4 days to find the desired network. Second, since the search process is hardware oblivious, neither the time performance nor the hardware efficiency can be guaranteed.

Recently, hardware-aware NAS [6]–[8] has been proposed to search architectures for a target hardware platform, as shown in Figure 1(a). They always assume a fixed hardware design (mobile chips) and only explore the architecture search space for fixed hardware. However, the hardware design freedom is commonly available in many cloud and edge computing applications, like FPGAs in cloud platforms [9], [10] and ASIC in edge computing platforms [13], [14]. Without the consideration of hardware design space will lead to inferior designs in hardware efficiency, because the hardware design space and the architecture search space are tightly coupled.

Compared with existing work, the main contribution of this work is to propose a framework to co-explore the architecture search space and the hardware design space, as shown in Figure 1(b). More specifically, this framework determines the best hardware during the search process, which is tailor-made for the candidate architectures. In this way, the framework can obtain a set of superior architecture and hardware design pairs on the Pareto frontier of accuracy and hardware efficiency tradeoffs. In addition, the search time can be significantly reduced, since we prune more inferior architectures according to multiple design specifications compared with the hardware-aware NAS.

B. Implementing DNNs on FPGAs

This paper will employ FPGA as a vehicle to study how to co-explore neural architectures and hardware designs.

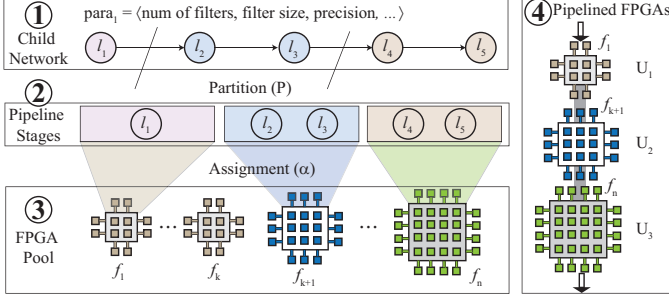


Figure 2. An overview of implementing a child network onto multiple FPGAs to be organized in the pipelined fashion.

FPGA has demonstrated its excellent ability to achieve high performance and energy efficiency for low-batch real-time inferences [18], [19]. Hence, a large amount of work is made in implementing neural networks on FPGAs, in which tools are developed to automatically design accelerators on FPGAs for a given network architecture. In the early stage, research efforts are mainly focusing on designing accelerators on a single FPGA [28]–[31]. Most recently, implementations on multiple FPGAs has become the mainstream [15], [18]–[20], [22], [23], since limited resource on a single FPGA becomes the performance bottleneck.

To fully utilize the computation power provided by multiple FPGAs, a typical technique is to implement the neural network on multiple FPGAs in a pipelined fashion [15], [20], [22], [23]. Figure 2 demonstrates one such example, in which a 5-layer network is partitioned into 3 pipeline stages, and each pipeline stage is mapped to a certain FPGA in an available pool. Finally, those FPGAs are connected as a linear array to function in the pipelined fashion.

C. Definitions and Problem Statement

The goal of the proposed framework is to find both the neural architectures with the highest test accuracy and hardware design with the guaranteed performance (e.g. timing requirement and utilization of FPGAs). In this subsection, we will first present the relevant system definitions. Then, we will formally define the problem based on FPGA.

① **Child Network.** A child network is defined as $C = \langle L, para, acc \rangle$. It consists of a set of layers L . The number of layers in the child network is the size of set L , i.e., $|L|$. For the i^{th} layer $l_i \in L$, set $para_i$ contains the predictable parameters, such as the number of filters, filter size, etc. The accuracy of the child network is acc , which can be obtained by training C on a held-out dataset. For illustration purposes, we use a linear chain of layers as an example in Figure 2 ①. However, the proposed technique is not limited to such structure and is applicable to more complicated structures, such as Directed Acyclic Graph (DAG).

The child network is the bridge between the architecture search space and the hardware design space. Specifically, in each iteration, the controller RNN will predict child networks from the architecture search space, and then determine their

implementations in the hardware design space. We will introduce the hardware design space as follows.

② **Partition Child Network to Pipeline Stages.** Let $P(C)$ be a set of partitions for the child network C . $P(C) = \{P_1, P_2, \dots, P_M\}$, where P_i is a nonempty subset of set L . We have the following two properties: (1) $\bigcup_{P_i \in P(C)} = L$; and (2) $\forall P_i, P_j \in P(C)$, if $i \neq j$, then $P_i \cap P_j = \emptyset$. After the partitioning, each set in $P(C)$ corresponds to a pipeline stage. For example, in Figure 2 ②, we partition the given child network into 3 pipeline stages, $P_1 = \{l_1\}$, $P_2 = \{l_2, l_3\}$, and $P_3 = \{l_4, l_5\}$.

③ **Assign Pipeline Stages to FPGAs.** Then, we can assign each pipeline stage to a specific FPGA in an available FPGA pool, as shown in Figure 2 ③. An FPGA pool with n FPGAs can be represented by a set $F = \{f_0, f_1, \dots, f_n\}$. Each FPGA, f_i , has a set of attributes, including memory mem_i , DSP slices dsp_i , etc. These attributes will be utilized to model the timing performance for a child network.

We define the assignment function α from the partition set $P(C)$ to FPGA pool F . We have $\alpha(P_i) = f_j$ to indicate the i^{th} pipeline stage P_i is assigned to the j^{th} FPGA f_j to be implemented. After pipeline stages are assigned to FPGA pool according to α , each FPGA will process one or multiple layers. And all FPGAs work together in the pipelined fashion.

④ **Pipelined FPGAs.** The pipelined executions of multiple FPGAs are illustrated in Figure 2 ④. The system will continuously obtain inputs from the dataset with a fixed rate (frame per second), and generate output data from the last pipeline stage. The input rate of the system reflects the throughput specification TS , which implies that the latency of each pipeline stage should be no more than $1/TS$.

The latency of a pipeline stage under an assignment function can be easily captured with a performance model [28]. For FPGA f_i , its latency is denoted as Lat_i . After obtaining the latency of each FPGA, we introduce pipeline efficiency, which is composed of the hardware utilization in each pipeline stage (corresponding to an FPGA). The utilization of FPGA f_i is equal to $Lat_i \times TS$. Higher utilization of an FPGA indicates the less idle time in processing and higher energy efficiency. Therefore, high average utilization of all FPGAs is always desired.

Problem Statement. Based on the above definitions, we formally define the problem of “hardware/software co-exploration of neural architectures” as: Given a dataset, a pool of FPGAs F , and a throughput specification TS , we are going to co-explore architecture search space and hardware design space to find a child network C :

- $para$: parameters of all layers in the child network;
- P : the partition of layer set L in the child network;
- α : the assignment of pipeline stages to set F ;

such that the accuracy of child network C is maximized, the pipeline FPGA system can meet the required throughput TS , and the average utilization of all FPGAs is maximized.

III. HW/SW CO-EXPLORATION FRAMEWORK

In this section, we will present the proposed framework. We will use the NAS discussed in [2] as the backbone framework

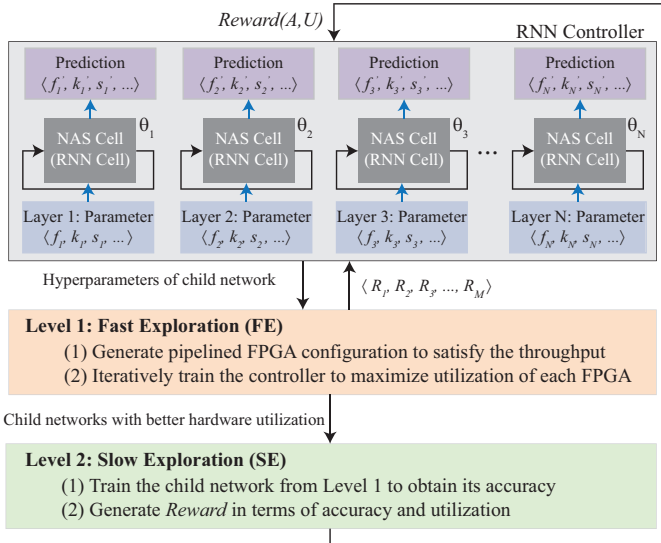


Figure 3. An overview of HW/SW co-exploration framework: The controller contains multiple reconfigurable RNN cells and predicts the hyperparameters in a child network; the fast exploration level prunes child networks with inferior hardware utilization; the slow exploration level updates controller using hardware utilization and accuracy obtained by training child networks.

and FPGA as the hardware platform to demonstrate our concept. It can be integrated with any existing NAS techniques [2], [8], [16], [17] or extended to incorporate other hardware platforms.

A. Framework Overview

Figure 3 shows the HW/SW co-exploration framework. The framework contains a RNN based controller and two levels of explorations. Unlike that in [2], the controller has multiple RNN cells instead of one. More specifically, each layer in a child network has a corresponding RNN cell. During the exploration, cells will be reorganized to support different optimization goals.

In the first level, a fast exploration is carried out in four steps: (1) it first predicts an architecture with probability p , (2) then, it explores the design space to generate a pipelined FPGA system to meet the throughput requirement, (3) according to the pipeline structure, it then reorganizes RNN cells in the controller, and (4) it updates the controller using reinforcement learning to maximize the pipeline efficiency. This level explores the hardware design space without training child networks, therefore it performs efficiently.

In the second level, we train the child network obtained from the first level on the held-out validation set. After that, we generate a reward based on both the yielded accuracy and pipeline efficiency, which is used to update the RNN controller. In case that no child network can meet the required throughput specification in the first level, we generate a negative reward to update the controller. After this level, the controller will predict a new child network from architecture search space for the fast exploration level.

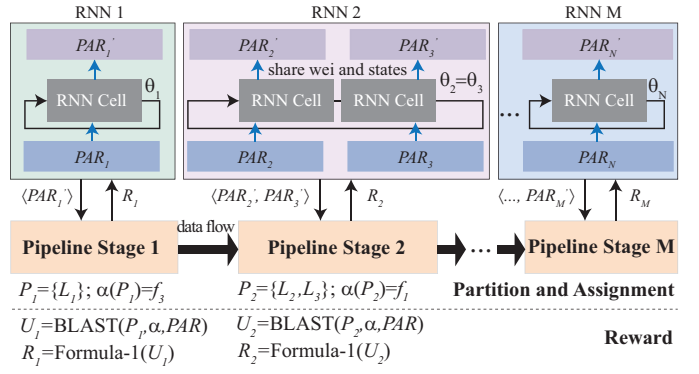


Figure 4. Fast Exploration (FE): organize RNN cells in the controller according to the partition for pipeline stages; independently update multiple RNNs in the controller to predict parameters of layers assigned to each pipeline stage.

B. Fast Exploration for High Resource Utilization

In the first level, namely Fast Exploration (FE), the objective is to maximize pipeline efficiency under the throughput specification TS . FE takes three types of inputs: (1) a set of available FPGAs F , (2) hyperparameters of a child network H , (3) a throughput specification TS . It will generate a new child network, whose throughput at inference phase can meet TS using a subset of FPGAs in F . In addition, the average hardware utilization of FPGAs can be maximized. In FE, there are two challenges needing to be addressed: first, how to partition a given child network and assign each partition to a specific FPGA (Partition and Assignment); second, how to reorganize the RNN cells in the controller and then update them to generate child networks with higher pipeline efficiency (Reorganize and Update Controller).

Partition and Assignment. In the search process, a number of candidate child networks need to go through the partition and assignment process. Consequently, an efficient automatic tool should be employed to avoid performance degradation on search process. In this paper, we employ the BLAST algorithm in [20]. BLAST takes child network H , FPGAs F , the throughput specification TS , and the attributes of each FPGA as inputs. It outputs a serial of FPGAs, each of which will implement one or multiple layers in a pipeline stage. The resultant system will satisfy TS with the maximum pipeline efficiency. As shown in Figure 4, layers in a child network are divided into M partitions, and each partition is assigned to one specific type of FPGA under function α .

Reorganize and Update Controller. According to the generated pipeline structure, we then reorganize the controller and iteratively update the controller to generate child networks with higher hardware utilization. Our goal is to maximize the average hardware utilization, which is equivalent to maximize the utilization of each hardware. However, the design space of maximizing the average hardware utilization is exponentially larger than that of maximizing the utilization of each hardware. To efficiently explore the design space, we choose to maximize the hardware utilization of different pipeline stage independently. Therefore, we reorganize RNN cells in the controller according to the determined pipeline structure. More

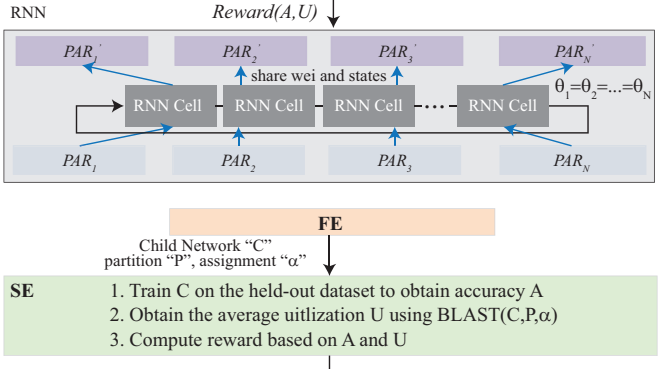


Figure 5. Slow Exploration (SE): configure RNN cells in the controller to be one RNN; generate reward based on accuracy and pipeline efficiency to update the controller RNN.

specifically, for multiple layers in one pipeline stage, their corresponding RNN cells will be configured to form one RNN and their weights and states are shared (e.g., RNN 2 in Figure 4). In consequence, there will be N RNNs for N pipeline stages. In this way, each RNN can be trained to maximize the hardware utilization for each FPGA pipeline stage.

After we form the RNNs, we apply reinforcement learning to update the parameters in those N RNNs, and use these RNNs to predict the hyperparameters of child networks. In each iteration, we will predict T child networks, which can be viewed as a list of actions $a_{1:T}$. Correspondingly, notation $a_{1:T}^i$ represents the hyperparameters of the i^{th} pipeline stage in these child networks. For each child network predicted by the controller, we can obtain the utilization of the i^{th} pipeline stage (corresponding to one FPGA) using BLAST, denoted as U_i . Then, for RNN i , we utilize U_i to generate a reward R_i to update its parameters θ_i . The reward R_i can be calculated using the following formula.

$$R_i = \begin{cases} U_i & U_i \leq 1 \\ 1 - U_i & 1 < U_i \leq 2 \\ -1 & U_i > 2 \end{cases} \quad (1)$$

where $U_i > 1$ indicates that the required throughput cannot be satisfied, and we give the negative reward. For each RNN, our objective is to maximize the expected reward for actions from time 1 to T , represented by $J(\theta_i) = E_{P(a_{1:T}^i; \theta_i)}[R_i]$. Since the reward is non-differentiable, we apply the policy of gradient method to update θ_i . Specifically, the method of REINFORCE rule [32] has been employed as in [2], [8].

C. Slow Exploration for High Accuracy

After obtaining a child network meeting the timing specification through the fast exploration level, we now move to the second level. In this level, we aim to update the controller RNN to generate new child networks with higher accuracy and pipeline efficiency. We will train the child network on the held-out validate set, and therefore the exploration speed is much slower than that of the first one. We call it Slow Exploration (SE).

As shown in Figure 5, SE takes the generated child network, the partition and the assignment from FE as the inputs. The

child network is first trained to obtain accuracy A . Then, the average pipeline efficiency U of the child network under the partition and assignment will be calculated. Finally, we compute the reward to update the controller using the following formula.

$$Reward(A, U) = \beta \times A + (1 - \beta) \times U \quad (2)$$

where β is an adjustment parameter, which reflects the bias on test accuracy and hardware utilization. The value of β ranges from 0 to 1. We will discuss how to scale β in Section V. After that, we update the controller using the reward by applying the policy gradient reinforcement learning, which is the same as that in FE level. As shown in Figure 5, all RNN cells share the same weights and states in this level, since we have only one reward.

D. Interface between Fast-Slow Explorations

Before updating the RNN cells in the controller in the fast exploration level, we take a snapshot *Snap* of all RNN cells. During the fast exploration level, we obtain the hardware design (i.e., pipeline configuration) for the input child network. Based on the determined pipeline structure, RNN cells are reorganized as introduced in Section III-B. And reorganized cells will be trained to generate better child networks for the previously obtained hardware design (i.e., pipeline configuration). Finally, a child network with maximum hardware efficiency on the determined pipeline will be sent to the slow exploration level.

After entering the slow exploration level, the RNN cells in the controller will be recovered using the previously saved snapshot *Snap*. Then, SE will train the child network to obtain the accuracy, which will be used to calculate the reward. Using this reward, we will update the recovered RNN. Then, the updated RNN will be used to generate new child networks for the next iteration. In this way, the SE process will always keep improving the RNN accuracy while the FE process will always generate the best hardware design for each iteration.

IV. EXPERIMENTS

Datasets: We use CIFAR-10 and ImageNet datasets to study the efficacy of our approach and compare it with the state-of-the-art. During the exploration of child networks, we only use the training images in these datasets, while the test images are used to test the accuracy of the resultant architectures. To evaluate the accuracy in the search process, we randomly select 10% of the samples from the training set as a validation set. All the images undergo the data preprocessing and augmentation procedure, including whitening, upsampling, random cropping, and random horizontal flip, which are common among the related work.

Architecture Search Space: For CIFAR-10, we use convolutional architectures as the backbone. For every convolutional layer, we first determine the filter size in [24, 36, 48, 64], the kernel size in [1, 3, 5, 7], and the strides. Two sets of experiments are carried out to determine the strides: (1) by exploring the child networks with a fixed stride of 1; (2) by allowing the controller to predict the strides in [1, 2]. After each layer, the

rectified linear units [33] and the batch normalization [34] are appended.

For ImageNet, the architecture repeats mobile inverted bottleneck convolution layers instead of ordinary convolutional ones, same as that in [8]. The controller explores the architectures with various kernel sizes [3,5,7], strides [1,2] and expansion ratios [3,6].

Hardware Design Space: The hardware design space is composed of up to three Xilinx FPGAs (XC7Z015), each of which contains 74K logic cells, 4.9Mb on-chip memory, and 150 DSP Slices. One reason for our selection is that such an FPGA provides high speed serial communication (up to 16.8Gbps of bandwidth), so that a high speed hardware pipeline can be formed by multiple FPGAs. In the implementation, the child network is partitioned into pipeline stages, and each stage is mapped to one FPGA. Kindly note that our hardware exploration may not end up using all three FPGAs; it is possible to use fewer for higher hardware efficiency.

In the experiments, we use pipeline efficiency as the metrics to measure the hardware efficiency. As stated in Section I, the pipeline efficiency is one of the most important metrics, since it is related to the hardware utilization, energy efficiency, and timing performance. Then, the timing specifications are set according to the desired processing speed of the data at the inference phase, which are commonly decided by the data collector (e.g., camera). For CIFAR-10, we set the throughput specification to 35FPS, which can satisfy most cameras; whereas for ImageNet, due to the more complicated architectures and the limited resource, we set the specification to 10FPS.

Exploration Frameworks: Our proposed framework is denoted as “Co-Exploration” in the results. The framework can obtain a set of superior architecture and hardware design pairs on the Pareto frontier of accuracy and pipeline efficiency tradeoffs. In particular, among the pairs on the frontier, we denote the one with the maximum accuracy as “OptSW” and the one with the maximum pipeline efficiency as “OptHW”.

For comparison, we also implement two other frameworks based on the state-of-the-art. Because none of the existing Hardware-Aware NAS [6]–[8] target FPGAs and they use various settings, for fair evaluation, we use the NAS discussed in [2] as the backbone to implement a Hardware-Aware NAS for FPGA under the same setting discussed above. This framework is denoted as Hardware-Aware NAS in the results. In addition, for the architectures obtained by the Hardware-Aware NAS, we further optimize their hardware implementation by considering the hardware design space. Such a heuristic approach is denoted as “Sequential Optimization” in the results.

Training Details: For CIFAR-10, the training settings for both the RNN controller and the child networks are the same as [2]. For the controller RNN, in both slow and fast explorations, it is trained by using the calculated rewards with the ADAM optimizer [35] with a learning rate of 0.0006. Parameter β in Formula 2 is set to 0.5 to equally optimize test accuracy and pipeline efficiency. For the child networks, we apply Momentum Optimizer with a learning rate of 0.1, weight decay of 10^{-4} , and momentum of 0.9. Each child network is trained for 50 epochs.

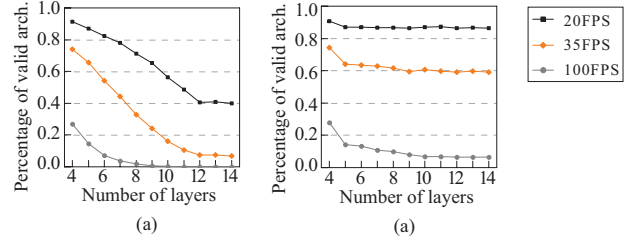


Figure 6. Percentages of valid architectures for different timing specifications: (a) fixed stride of 1; (b) predictable strides.

Table II
CO-EXPLORATION WITH PREDICTABLE STRIDE PERFORMS BETTER THAN THAT WITH FIXED STRIDE UNDER 35FPS TIMING SPECIFICATION.

Models	Depth	Accuracy	Pipeline Eff.
Co-Exploration fixed stride (OptSW)	13	81.50%	91.92%
Co-Exploration fixed stride (OptHW)	10	78.57%	98.56%
Co-Exploration pred. stride (OptSW)	14	85.19%	92.15%
Co-Exploration pred. stride (OptHW)	6	80.18%	99.69%

For ImageNet, we build the distributed GPU training environment on top of Uber Horovod [36]. Training settings are similar to those for CIFAR-10, with the exceptions that we set the initial learning rate to 0.0125, decay $10\times$ at selected epochs, and for the Momentum Optimizer the weight decay is 5×10^{-5} and the momentum is 0.9.

V. RESULTS

Impact of Timing Specifications: Figure 6 reports the impact of timing specifications for the Co-Exploration framework. We randomly sample 10,000 architectures for the layer size ranged from 4 to 14, and obtain the percentage of valid architectures that can meet the timing specification on the CIFAR-10 dataset. In Figure 6, it is obvious that if the constraint is tight (e.g., FPS=100), only a few architectures can satisfy the specification, indicating that the number of architectures with high accuracy is reduced compared with the one without timing constraints. In this case, we can scale up the parameter β in Formula 2 to pursue higher accuracy. On the other hand, if the constraint is loose (e.g., FPS=20), there are a large number of valid architectures. Correspondingly, we can scale down β to find more hardware efficient designs with high accuracy.

Comparison between Fixed Stride and Predictable Stride: Table II reports the comparison between the exploration with the fixed stride and that with the predictable stride on CIFAR-10. In the table, column “depth” indicates the number of layers in the resulting architecture. As shown in this table, for the exploration with the fixed stride, OptSW achieves 2.93% higher accuracy but 6.64% loss in pipeline efficiency than OptHW. These figures are 5.01% and 7.54% for the exploration with the predictable strides. In addition, it is obvious that compared with fixed stride, the stride prediction can help controller to find better results in both accuracy and pipeline efficiency. As such, in the following experiments

Table III

COMPARISON AMONG CO-EXPLORATION, HARDWARE-AWARE NAS AND SEQUENTIAL OPTIMIZATION ON CIFAR-10 AND IMAGENET DATASETS.

Dataset	Models	Depth	Parameters	Accuracy (Top1)	Accuracy (Top5)	Pipeline Eff.	FPS	Energy Eff. GOPS/W
CIFAR-10	Hardware-Aware NAS	13	0.53M	84.53%	-	73.27%	16.2	0.84
	Sequential Optimization	13	0.53M	84.53%	-	92.20%	29.7	1.36
	Co-Exploration (OptHW)	10	0.48M	78.57%	-	98.56%	35.5	2.55
	Co-Exploration (OptSW)	14	0.36M	85.19%	-	92.15%	35.5	1.91
ImageNet	Hardware-Aware NAS	15	0.44M	68.40%	89.84%	81.07%	6.8	0.34
	Sequential Optimization	15	0.44M	68.40%	89.84%	86.75%	10.4	0.46
	Co-Exploration (OptHW)	17	0.54M	68.00%	89.60%	96.15%	12.1	1.01
	Co-Exploration (OptSW)	15	0.48M	70.24%	90.53%	93.89%	10.5	0.74

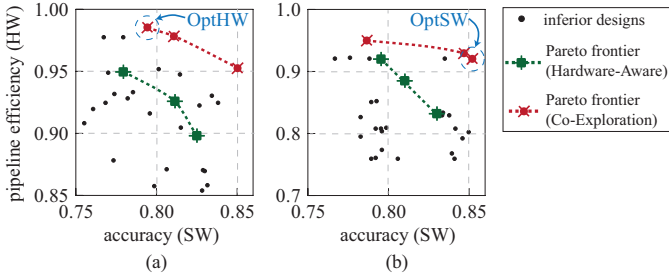


Figure 7. Pareto frontiers between accuracy and pipeline efficiency for Hardware-Aware NAS and Co-Exploration, both of which are designed under the timing specification of 35FPS: (a) designs with 2 FPGAs; (b) designs with 3 FPGAs.

we will use predictable stride as the default setting for Co-Exploration.

Impact of Different Exploration Frameworks on Pareto Frontier:

Figure 7 reports the design space exploration assuming the hardware design space contains up to (a) two FPGAs or (b) three FPGAs. The x-axis and y-axis represent the accuracy and pipeline efficiency, respectively. For clear demonstration, we only include the architectures whose pipeline efficiency is no less than 85% for two FPGAs in Figure 7(a) and no less than 75% for three FPGAs in Figure 7(b). In these figures, the circled design points correspond to those in Table II. The red lines represent the Pareto frontiers explored by Co-Exploration. The green lines, on the other hand, represent the frontier obtained by Hardware-Aware NAS (by examining the top architectures identified). These figures clearly show that by exploring hardware design space, our Co-Exploration can significantly push forward the Pareto frontiers in the accuracy and efficiency tradeoffs. It effectively identifies better designs not available through architecture search space only, i.e., those between the two frontiers.

Comparing the two exploration results in Figure 7(a) and (b), we can also see that the solution with the highest pipeline efficiency is located in Figure 7(a), while the one with the highest accuracy is located in Figure 7(b). In general, we can always observe that the average accuracy on three FPGAs is higher than that on two FPGAs, yet the pipeline efficiency is lower. This is because more FPGAs can accommodate deeper architecture in layers for higher accuracy. On the other hand,

Table IV
CO-EXPLORATION USES MUCH FEWER GPU HOURS THAN THAT OF HARDWARE-AWARE NAS, BENEFITING FROM THE EARLY-STAGE PRUNING.

Dataset	Approach	Arch for Training	GPU Hours	Impr.
CIFAR-10	Hardware-Aware NAS	108,000	16,586	1
	Co-Exploration	308	$102+1.9=103.9$	$159\times$
ImageNet	Hardware-Aware NAS	7,263	36,315	1
	Co-Exploration	53	$256+1.8=266.8$	$136\times$

more layers will easily result in unbalanced pipeline stages, which in turn reduces the pipeline efficiency.

Comparison between Co-Exploration and Existing Frameworks:

Table III reports the comparison results on accuracy, pipeline efficiency, throughput and energy efficiency on CIFAR-10 and ImageNet. All the architectures identified have fewer than 1M parameters mainly due to the hardware capacity. This inevitably leads to accuracy loss; however, as we can see, the architecture explored by OptSW can still achieve 85.19% test accuracy on CIFAR-10, and 70.24% top-1 accuracy on ImageNet. These results demonstrate the effectiveness of the Co-Exploration approach in resource limited scenarios. In addition, OptSW outperforms Hardware-Aware NAS by achieving 54.37% and 35.24% higher throughput, and 56.02% and 54.05% higher energy efficiency on CIFAR-10 and ImageNet, respectively. Compared with Sequential Optimization, OptSW achieves 16.34% and 28.79% improvements on CIFAR-10 in throughput and energy efficiency, respectively; and on ImageNet, it can also slightly improve throughput, and achieve 37.84% improvements on energy efficiency.

Finally, Table IV reports the comparison results on normalized search time between the Hardware-Aware NAS and the Co-Exploration. Results in this table show that the Co-Exploration can significantly accelerate the search process, achieving 159 \times and 136 \times fewer GPU hours on CIFAR-10 and ImageNet, respectively. The speedup is achieved from the efficient early-stage pruning in the fast exploration level. First, many inferior architectures can be pruned, such that the number of architectures needing to be trained is significantly reduced, as shown in column “Arch for Training”. Second, the exploration of the hardware design space is efficient, which only occupies less than 1% GPU hours in the whole search process (1.9 GPU hours for CIFAR-10 and 1.8 GPU hours for

ImageNet).

VI. CONCLUSION

We proposed the co-exploration framework to open up the hardware design freedom in neural architecture search. This is driven by the trend that the hardware platform can be programmed or even fully customized for the best performance in cloud and edge computing applications. This paper took the FPGA as a vehicle to show that through jointly exploring architecture search space and hardware design space, the design Pareto frontier on accuracy and hardware efficiency tradeoffs can be significantly pushed forward. For future work, we would like to conduct experiments on other tasks, such as object detection and tracking, speech recognition, etc. In addition, we will identify and study the challenges in integrating ASIC designs to the proposed co-exploration framework for NAS.

REFERENCES

- [1] H. Cai, T. Chen, W. Zhang, Y. Yu, and J. Wang, “Efficient architecture search by network transformation.” *AAAI*, 2018.
- [2] B. Zoph and Q. V. Le, “Neural architecture search with reinforcement learning,” in *International Conference on Learning Representations (ICLR)*, 2017.
- [3] B. Zoph, V. Vasudevan, J. Shlens, and Q. V. Le, “Learning transferable architectures for scalable image recognition,” in *IEEE conference on Computer Vision and Pattern Recognition (CVPR)*, 2018, pp. 8697–8710.
- [4] E. Real, S. Moore, A. Selle, S. Saxena, Y. L. Suematsu, J. Tan, Q. Le, and A. Kurakin, “Large-scale evolution of image classifiers,” *arXiv preprint arXiv:1703.01041*, 2017.
- [5] H. Liu, K. Simonyan, O. Vinyals, C. Fernando, and K. Kavukcuoglu, “Hierarchical representations for efficient architecture search,” *arXiv preprint arXiv:1711.00436*, 2017.
- [6] B. Wu, X. Dai, P. Zhang, Y. Wang, F. Sun, Y. Wu, Y. Tian, P. Vajda, Y. Jia, and K. Keutzer, “Fbnnet: Hardware-aware efficient convnet design via differentiable neural architecture search,” *arXiv preprint arXiv:1812.03443*, 2018.
- [7] M. Tan, B. Chen, R. Pang, V. Vasudevan, and Q. V. Le, “Mnasnet: Platform-aware neural architecture search for mobile,” *arXiv preprint arXiv:1807.11626*, 2018.
- [8] H. Cai, L. Zhu, and S. Han, “Proxylessnas: Direct neural architecture search on target task and hardware,” *arXiv preprint arXiv:1812.00332*, 2018.
- [9] Amazon, “Ec2 f1 instances,” <https://aws.amazon.com/ec2/instance-types/f1>, 2017, accessed: 2019-01-20.
- [10] Microsoft, “Real-time ai: Microsoft announces preview of project brainwave,” <https://blogs.microsoft.com/ai/build-2018-project-brainwave/>, 2018, accessed: 2019-01-20.
- [11] J. Wang, Q. Lou, X. Zhang, C. Zhu, Y. Lin, and D. Chen, “Design flow of accelerating hybrid extremely low bit-width neural network in embedded fpga,” in *2018 28th International Conference on Field Programmable Logic and Applications (FPL)*. IEEE, 2018, pp. 163–1636.
- [12] F. Shafiq, T. Yamada, A. T. Vilchez, and S. Dasgupta, “Automated flow for compressing convolution neural networks for efficient edge-computation with fpga,” *arXiv preprint arXiv:1712.06272*, 2017.
- [13] S. Venkataramani, A. Ranjan, S. Banerjee, D. Das, S. Avancha, A. Jaganathan, A. Durg, D. Nagaraj, B. Kaul, P. Dubey *et al.*, “Scaleddeep: A scalable compute architecture for learning and evaluating deep networks,” in *ACM SIGARCH Computer Architecture News*, vol. 45, no. 2. ACM, 2017, pp. 13–26.
- [14] P. Whatmough, S. Lee, N. Mulholland, P. Hansen, S. Kodali, D. Brooks, and G. Wei, “Dnn engine: A 16nm sub-uj deep neural network inference accelerator for the embedded masses,” in *2017 IEEE Hot Chips 29 Symposium*, 2017.
- [15] C. Zhang, D. Wu, J. Sun, G. Sun, G. Luo, and J. Cong, “Energy-efficient cnn implementation on a deeply pipelined fpga cluster,” in *International Symposium on Low Power Electronics and Design (ISLPED)*. ACM, 2016, pp. 326–331.
- [16] H. Liu, K. Simonyan, and Y. Yang, “Darts: Differentiable architecture search,” *arXiv preprint arXiv:1806.09055*, 2018.
- [17] G. Bender, P.-J. Kindermans, B. Zoph, V. Vasudevan, and Q. Le, “Understanding and simplifying one-shot architecture search,” in *International Conference on Machine Learning*, 2018, pp. 549–558.
- [18] E. Chung, J. Fowers, K. Ovtcharov, M. Papamichael, A. Caulfield, T. Massengill, M. Liu, D. Lo, S. Alkalay, M. Haselman *et al.*, “Serving dnns in real time at datacenter scale with project brainwave,” *IEEE Micro*, vol. 38, no. 2, pp. 8–20, 2018.
- [19] J. Fowers, K. Ovtcharov, M. Papamichael, T. Massengill, M. Liu, D. Lo, S. Alkalay, M. Haselman, L. Adams, M. Ghandi *et al.*, “A configurable cloud-scale dnn processor for real-time ai,” in *International Symposium on Computer Architecture (ISCA)*. IEEE, 2018, pp. 1–14.
- [20] W. Jiang, E. H.-M. Sha, Q. Zhuge, L. Yang, X. Chen, and J. Hu, “Heterogeneous fpga-based cost-optimal design for timing-constrained cnns,” *IEEE Transactions on Computer-Aided Design of Integrated Circuits and Systems*, vol. 37, no. 11, pp. 2542–2554, 2018.
- [21] W. Zhang, J. Zhang, M. Shen, G. Luo, and N. Xiao, “An efficient mapping approach to large-scale dnns on multi-fpga architectures,” in *Design, Automation & Test in Europe Conference & Exhibition (DATE)*, 2019. IEEE, 2019, pp. 1–4.
- [22] T. Geng, T. Wang, A. Sanaullah, C. Yang, R. Patel, and M. Herboldt, “A framework for acceleration of cnn training on deeply-pipelined fpga clusters with work and weight load balancing,” in *International Conference on Field Programmable Logic and Applications (FPL)*. IEEE, 2018, pp. 394–3944.
- [23] T. Geng, T. Wang, A. Sanaullah, C. Yang, R. Xu, R. Patel, and M. Herboldt, “Fpdeep: Acceleration and load balancing of cnn training on fpga clusters,” in *International Symposium on Field-Programmable Custom Computing Machines (FCCM)*. IEEE, 2018, pp. 81–84.
- [24] J. D. Schaffer, D. Whitley, and L. J. Eshelman, “Combinations of genetic algorithms and neural networks: A survey of the state of the art,” in *International Workshop on Combinations of Genetic Algorithms and Neural Networks (COGANN)*. IEEE, 1992, pp. 1–37.
- [25] B. Baker, O. Gupta, N. Naik, and R. Raskar, “Designing neural network architectures using reinforcement learning,” *arXiv preprint arXiv:1611.02167*, 2016.
- [26] L. Xie and A. Yuille, “Genetic cnn,” in *International Conference on Computer Vision (ICCV)*. IEEE, 2017, pp. 1388–1397.
- [27] Y.-H. Kim, B. Reddy, S. Yun, and C. Seo, “Nemo: Neuro-evolution with multiobjective optimization of deep neural network for speed and accuracy,” in *ICML 2017 AutoML Workshop*, 2017.
- [28] C. Zhang, P. Li, G. Sun, Y. Guan, B. Xiao, and J. Cong, “Optimizing fpga-based accelerator design for deep convolutional neural networks,” in *International Symposium on Field-Programmable Gate Arrays (FPGA)*. ACM, 2015, pp. 161–170.
- [29] Y. Shen, M. Ferdman, and P. Milder, “Maximizing cnn accelerator efficiency through resource partitioning,” in *International Symposium on Computer Architecture (ISCA)*. IEEE, 2017, pp. 535–547.
- [30] X. Zhang, J. Wang, C. Zhu, Y. Lin, J. Xiong, W.-m. Hwu, and D. Chen, “Dnnbuilder: An automated tool for building high-performance dnn hardware accelerators for fpgas,” in *International Conference on Computer-Aided Design (ICCAD)*. ACM, 2018, p. 56.
- [31] X. Wei, Y. Liang, X. Li, C. H. Yu, P. Zhang, and J. Cong, “Tgpa: tile-grained pipeline architecture for low latency cnn inference,” in *International Conference on Computer-Aided Design (ICCAD)*. IEEE, 2018, pp. 1–8.
- [32] R. J. Williams, “Simple statistical gradient-following algorithms for connectionist reinforcement learning,” *Machine learning*, vol. 8, no. 3–4, pp. 229–256, 1992.
- [33] V. Nair and G. E. Hinton, “Rectified linear units improve restricted boltzmann machines,” in *International Conference on Machine Learning (ICML)*, 2010, pp. 807–814.
- [34] S. Ioffe and C. Szegedy, “Batch normalization: Accelerating deep network training by reducing internal covariate shift,” *arXiv preprint arXiv:1502.03167*, 2015.
- [35] D. P. Kingma and J. Ba, “Adam: A method for stochastic optimization,” *arXiv preprint arXiv:1412.6980*, 2014.
- [36] A. Sergeev and M. Del Balso, “Horovod: fast and easy distributed deep learning in tensorflow,” *arXiv preprint arXiv:1802.05799*, 2018.